Published in final edited form as:
Immunity. 2009 October 16; 31(4): 598–608. doi:10.1016/j.immuni.2009.07.007.

Distinct Conformations of Ly49 Natural Killer Cell Receptors Mediate MHC Class I Recognition in *Trans* and *Cis*

Jonathan Back[1,4], **Emilio L. Malchiodi**[2,4], **Sangwoo Cho**[2,4], **Léonardo Scarpellino**[1], **Pascal Schneider**[3], **Melissa C. Kerzic**[2], **Roy A. Mariuzza**[2,5], and **Werner Held**[1,5]

[1]Ludwig Institute for Cancer Research Ltd., Lausanne Branch and University of Lausanne, 1066 Epalinges, Switzerland [2]Center for Advanced Research in Biotechnology, W.M. Keck Laboratory for Structural Biology, University of Maryland Biotechnology Institute, Rockville, MD 20850, USA [3]Department of Biochemistry, University of Lausanne, 1066 Epalinges, Switzerland

Summary

Certain cell surface receptors engage ligands expressed on juxtaposed cells, but also ligands on the same cell. The structural basis for *trans* versus *cis* binding is not known. Here, we show that Ly49 natural killer (NK) cell receptors bind two MHC class I (MHC-I) molecules in *trans* when the two ligand-binding domains are back-folded onto the long stalk region. In contrast, dissociation of the ligand-binding domains from the stalk and their reorientation relative to the NK cell membrane allow monovalent binding of MHC-I in *cis*. The distinct conformations (back-folded and extended) define the structural basis for *cis–trans* binding by Ly49 receptors and explain the divergent functional consequences of *cis* versus *trans* interactions. Further analyses identified specific stalk segments that were not required for MHC-I binding in *trans*, but were essential for inhibitory receptor function. These data identify multiple distinct roles of stalk regions for receptor function.

Introduction

Cell surface receptors allow cell-to-cell communication by interacting with ligands expressed on other cells (*trans* interaction). Certain receptors can also engage ligands expressed on the same cell (*cis* interaction) (Held and Mariuzza, 2008). The molecular basis for *cis* versus *trans* binding is currently unknown. Here we have investigated the structural requirements for *cis–trans* interactions by Ly49 receptors, which allow natural killer (NK) cells to detect diseased cells.

NK cells are activated upon encounter with most normal cells. However, activation signaling is interrupted when inhibitory NK cell receptors engage major histocompatibility complex class I (MHC-I) molecules on other cells. This dual receptor system enables NK cells to detect virally infected or transformed cells with reduced levels of MHC-I molecules, i.e. cells which fail to trigger inhibitory MHC-I receptors. In this case NK cell activation can proceed and bring about target cell lysis, which is known as “missing-self” recognition.

5Correspondence: R.A.M. (mariuzza@carb.nist.gov; phone (240) 314 6243; fax (240) 314-6225) or W.H. (Werner.Held@licr.unil.ch; phone +41 21 692 5958; fax +41 21 692 5995).
[4]These authors contributed equally to this work.

Inhibitory MHC-I receptors include human leukocyte immunoglobulin (Ig)-like receptors (LILRs) and their orthologues, mouse paired Ig-like receptors (PIRs), killer Ig-like receptors (KIRs) (human), C-type lectin-like Ly49 receptors (mouse), and CD94–NKG2A receptors (human and mouse) (Lanier, 2005). Engagement of these receptors by MHC-I on prospective target cells leads to the recruitment of phosphatases such as SHP-1 (Burshtyn et al., 1996; Nakamura et al., 1997) and the adaptor molecule Crk (Peterson and Long, 2008), which counteract NK cell activation. Additionally, KIR and Ly49 receptors "educate" developing NK cells, i.e. they establish and maintain functional competence of NK cell activation pathways (Anfossi et al., 2006; Chalifour et al., 2009; Fernandez et al., 2005; Kim et al., 2005).

In addition to the inhibitory interaction with MHC-I on juxtaposed membranes, members of the Ly49 and LILRB/PIR receptor families can also bind MHC-I molecules in the plane of the same membrane (in *cis*) (Doucey et al., 2004; Masuda et al., 2007; Scarpellino et al., 2007). While *cis*-associated PIR-B delivers tonic inhibition signals (Masuda et al., 2007), there is no evidence that *cis* engagement of Ly49s results in inhibitory signalling (Doucey et al., 2004). Rather, a significant fraction of Ly49 receptors becomes unavailable for *trans* interaction (Back et al., 2007). Consequently, *cis* interaction reduces the inhibitory capacity of Ly49 and lowers the threshold at which the NK cells activation exceeds inhibition. In addition, *cis* interaction of Ly49A is required for NK cell education (Chalifour et al., 2009).

It is not known how cell surface receptors like Ly49 can bind MHC-I expressed in *cis* and *trans*, and why the two types of interactions have distinct functional outcomes. Ly49s are homodimeric type II glycoproteins, with each chain composed of a ligand-binding C-type lectin-like domain, termed the natural killer receptor domain (NKD), connected by a stalk of approximately 70 residues to the transmembrane and cytoplasmic domains (Deng and Mariuzza, 2006; Natarajan et al., 2002). Crystal structures of Ly49–MHC-I complexes have shown that Ly49s engage MHC-I at a broad cavity beneath the peptide-binding platform formed by the α1, α2 and α3 domains, and β_2-microglobulin (β_2m) (Dam et al., 2003; Deng et al., 2008; Tormo et al., 1999). Because *trans* and *cis* interactions utilize the same binding site (Doucey et al., 2004), Ly49 receptors must likely reverse the orientation of their ligand-binding domains relative to the NK cell surface in order to bind MHC-I in *trans* versus *cis*. If so, the exceptionally long stalk region of Ly49s, for which there is currently no structural information, may be crucial to support two orientations of the NKDs. In addition, structures of Ly49–MHC-I complexes revealed two modes of MHC-I engagement. In the Ly49C–H-2K^b complex (Dam et al., 2003; Deng et al., 2008), the Ly49C homodimer engages H-2K^b bivalently, such that each NKD makes identical interactions with MHC-I to form a symmetrical, butterfly-shaped assembly. By contrast, in the Ly49A–H-2D^d complex (Tormo et al., 1999), the Ly49A dimer contacts H-2D^d asymmetrically, with only one of its two subunits binding a single MHC-I molecule. The very different modes of MHC-I engagement are based on different geometries of the Ly49C and Ly49A dimers. The Ly49C dimer adopts an "open" conformation, while the Ly49A dimer adopts a "closed" conformation. Steric clashes preclude the closed Ly49A dimer from binding simultaneously two MHC-I molecules. However, a nuclear magnetic resonance study of unbound Ly49A revealed that in solution the receptor exists predominantly in the "open" state and that this form of Ly49A can bind two MHC-I molecules (Dam et al., 2006). Collectively, these data raise the possibility that *cis–trans* interactions are mediated by distinct Ly49 conformations (Held and Mariuzza, 2008).

To elucidate the basis for *cis* versus *trans* engagement of MHC-I by Ly49s, we determined the crystal structure of Ly49L in the absence and presence of a significant portion of the stalk region. This information was used to construct, and experimentally test, models of *cis* and *trans* Ly49–MHC-I complexes. This study, which represents the first comprehensive structure–function analysis of receptor interactions in *cis* versus *trans*, highlights how stalk regions can play essential roles in the function cell surface receptors.

Results

Structure of Ly49L NKD

The structure of Ly49L NKD was determined to 2.0 Å resolution (Table S1, Figure 1A). Like other Ly49 NKDs (Dam et al., 2003;Deng et al., 2008;Tormo et al., 1999), the Ly49L NKD adopts a fold consisting of two α-helices (α1 and α2) and two anti-parallel β-sheets (β0, β1, β5 and β2, β2′, β3, β4), including four intramolecular disulfide bonds (Figure 1A,D). The two monomers in the asymmetric unit form a dimer that closely resembles the Ly49A dimer (Figure 1B,E) (Tormo et al., 1999).

Superposition of Ly49L NKD on other Ly49 NKD structures (Deng et al., 2008; Tormo et al., 1999) yielded root-mean-square (r.m.s.) differences of 0.9 Å, 1.2 Å and 2.2 Å for Ly49A, Ly49G and Ly49C, respectively, suggesting that Ly49L is more closely related to Ly49A or Ly49G than to Ly49C. Indeed, although Ly49L is an activating receptor, it is structurally more similar to the inhibitory receptor Ly49A (or Ly49G) than is Ly49A to Ly49C, another inhibitory receptor. We therefore conclude that activating and inhibitory Ly49s are distinguished not by the structure of their NKDs, but by whether their cytoplasmic regions contain ITIM motifs or are associated with DAP12, respectively. The main structural difference between Ly49L and Ly49C is in loop L3, which contacts MHC-I in the Ly49A–H-2D^d and Ly49C–H-2K^b complexes and is a key determinant of MHC binding specificity (Deng et al., 2008). This loop is continuous in Ly49L, Ly49A and Ly49G (Figure 1A,B), but is interrupted by an α-helix (α3) in Ly49C (Figure 1C,F).

At the NK cell surface, Ly49 receptors exist as homodimers (Natarajan et al., 2002). In the crystal, the Ly49L dimer shows a similar subunit arrangement as Ly49A in the Ly49A–H-2D^d complex (Tormo et al., 1999), which we term the “closed” conformation, since the α2 helices of the NKDs are juxtaposed across the dimer interface (Figure 1A,B). In addition, the two subunits interact through strand β0, creating an extended anti-parallel β-sheet, with six main chain–main chain hydrogen bonds linking the strands (Figure S1A). This conformation is distinct from the “open” conformation of Ly49C and Ly49G (Dam et al., 2003; Deng et al., 2008), in which the α2 helices make no contacts (Figure 1C).

Structure of Ly49L with Stalk Region

Previous structural studies of Ly49 receptors have not provided any information on the stalk region connecting the NKD to the cell membrane (Held and Mariuzza, 2008). To visualize the stalk, and define its orientation relative to the NKD, we expressed various versions of the extracellular portion of several Ly49s, including Ly49A, Ly49C and Ly49L. However, only the extracellular portion of Ly49L (Ly49L-EC; residues 79–265), comprising the NKD and most of the stalk, could be crystallized. The structure was determined to 2.5 Å resolution (Table S1, Figure 2A). The four monomers in the asymmetric unit (designated A–D) form two homodimers (AB and CD). Superposition of the four monomers gave r.m.s. deviations in α-carbon positions of 0.5–0.8 Å, indicating close similarity. Accordingly, the following description of Ly49L-EC is based on monomer A, and that of the Ly49L-EC homodimer on monomers A and B, unless stated otherwise.

Although SDS-PAGE analysis of dissolved crystals confirmed the presence of an intact stalk, we could only detect electron density for the C-terminal 41 residues of the 68 stalk residues in the expressed protein, implying mobility of the N-terminal portion. In each Ly49L-EC monomer, the stalk is composed of an α-helix ($\alpha3_S$; residues Arg111–Lys132) and a loop (L_S; residues Thr133–Gly144) connecting the helix to the NKD (Figure 2). However, rather than projecting from the NKD as might be expected for a stalk region, the Ly49L stalk is back-folded onto the NKD. In the Ly49L-EC dimer, the stalks are linked by an N-terminal disulfide

bond (Cys110–Cys110) (Figure 2A). The $\alpha3_S$ helices of the stalks lie in long grooves at the junction between NKD subunits (Figure 2B), such that each helix makes numerous interactions with both NKDs (Table S2). By contrast, the $\alpha3_S$ helices do not contact each other, except at their N-termini (Figure 2C). Hence, the $\alpha3_S$ helices may be regarded as two blades of an open pair of scissors, whose pivot is the Cys110–Cys110 disulfide.

Parts of loop L_S, which links $\alpha3_S$ to the NKD, are disordered in monomers B and D in the asymmetric unit of the Ly49L-EC crystal. Moreover, L_S adopts significantly different conformations in monomers A and C, where it is completely ordered (r.m.s. deviation of 2.5 Å for 12 α-carbon pairs). Thus, the L_S loop, along with the Cys110–Cys110 pivot, may confer flexibility to the stalk region at specific points that could be important for Ly49 function. Based on these results, we carried out sequence comparisons and secondary structure predictions of Ly49 stalk regions (residues 110–144) (Figure S2A). This analysis revealed that Ly49L likely exemplifies other Ly49s, both in the structure of the stalk region and its disposition relative to the NKD. First, residues 111–132 are predicted to be α-helical in all cases, in excellent agreement with the Ly49L-EC crystal structure where they compose helix $\alpha3_S$. Second, residues 133–144 are predicted as random coil in all Ly49s, again consistent with the Ly49L-EC structure in which they form the flexible L_S loop. Third, Cys110 is conserved in 21 of 23 Ly49 family members (the sole exceptions, Ly49F and Ly49S, contain serine at this position), suggesting that the $\alpha3_S$ helices are typically disulfide-linked at their N-termini. Fourth, examination of the Ly49L-EC structure showed that NKD-contacting residues of the stalk region are well conserved among Ly49s, as are the NKD residues with which they interact. For example, of the 15 $\alpha3_S$ residues that contact the Ly49L NKD, 11 are identical in Ly49A and one is substituted conservatively (Lys/Arg122). In addition, a number of interaction pairs are strictly, or highly, conserved across the entire Ly49 family, including NKD Trp149–$\alpha3_S$ Thr131, NKD Tyr152–$\alpha3_S$ Glu/Asp123, NKD Glu188–$\alpha3_S$ Glu/Asp123, NKD Phe191–$\alpha3_S$ Leu/Ile120, and NKD Phe191–$\alpha3_S$ Leu/Ser116 (Table S2). Hence, it appears probable that stalk regions can generally back-fold onto Ly49 NKD dimers as observed in the Ly49C-EC structure (Figure 2).

Comparison of the Ly49L NKD and Ly49L-EC Dimers

The most notable difference between the Ly49L NKD and Ly49L-EC structures, apart from the presence of the stalk region in the latter, is the relative orientation of the NKD subunits composing the two homodimers. As indicated above, the Ly49L NKD dimer adopts a closed conformation (Figure 1A). By contrast, the Ly49L-EC dimer assumes an open conformation, such that the α2 helices do not interact (Figure 2A). The closed conformation is incompatible with a back-folded stalk, since the $\alpha3_S$ helices of the stalks occupy the gap between the α2 helices of the NKDs, effectively opening up the Ly49L dimer by ~20° compared to the closed state. Concomitantly, the register between β0 strands in the Ly49L4 dimer interface is shifted by four residues, reducing the number of main chain–main chain hydrogen bonds between the strands from six to four (Figure S1A,B). Thus, at least some Ly49s can adopt both open and closed states, which may correlate with *trans* and *cis* binding to MHC-I (see below).

A critical question is whether the open dimer observed in the Ly49L-EC structure, with its back-folded stalk region, is compatible with MHC-I recognition. Because the MHC specificity of Ly49L is unknown, we cannot measure ligand binding. However, the dimerization mode of Ly49L-EC closely resembles that of Ly49C in the Ly49C–H-$2K^b$ complex (Dam et al., 2003), with an r.m.s. difference in α-carbon positions of 1.71 Å between the two Ly49 dimers. Least-squares superposition of the Ly49L-EC and Ly49C–H-$2K^b$ structures showed that Ly49L, like Ly49C, could engage two MHC-I molecules, with some potential contacts, but no significant steric collisions, between the back-folded stalks and MHC-I (Figure 3A).

Model for *Trans* and *Cis* Interactions of Ly49 Receptors with MHC-I

We propose a model for *cis–trans* engagement of MHC-I by Ly49s that integrates all the available crystal structures (Dam et al., 2003; Deng et al., 2008; Tormo et al., 1999). Because *trans* and *cis* interactions utilize the same binding site beneath the peptide-binding platform of MHC-I (Doucey et al., 2004), Ly49 receptors must drastically reorient their NKDs relative to the NK cell membrane to bind MHC-I in *trans* versus *cis*. It is most likely that the exceptionally long stalk regions of Ly49s provide the requisite flexibility. In the modeled Ly49–MHC-I complex constructed using the Ly49L-EC and Ly49C–H-2K^b structures (Figure 3A), the N-termini of the stalks point in a direction completely opposite from the C-termini of the MHC-I molecules. In this view, the two MHC-I stand on the target cell surface at the bottom and the Ly49 dimer reaches MHC-I from an opposing NK cell above, to which it is tethered via back-folded stalks. Accordingly, we propose that the Ly49L-EC structure represents the conformation Ly49s assume to bind MHC-I in *trans*. Conversely, *cis* binding would require the stalks to assume an extended conformation that orients the NKDs with their N-termini towards the NK cell (Figure 3B). In contrast to the *trans* interaction, in which one Ly49 dimer binds two MHC-I molecules (Figure 3A), this model predicts that *cis* engagement of both NKDs by MHC-I is unlikely, due to the orientation that binding of one MHC-I molecule would impose on the Ly49 dimer (Figure 3B). If so, the bivalent Ly49C–H-2K^b and monovalent Ly49A–H-2D^d complexes would exemplify *trans* and *cis* recognition, respectively.

Stoichiometry of Ly49A–D^d *Cis* and *Trans* Complexes

Since the biological relevance of bivalent and monovalent MHC-I binding was unclear, we determined the stoichiometry of Ly49–MHC-I complexes on cell surfaces. Because the MHC-I specificity of Ly49L is not known, we used the highly homologous Ly49A receptor, which binds H-2D^d (D^d) but not D^b or K^b molecules, both in *trans* (Karlhofer et al., 1992) and in *cis* (Doucey et al., 2004). To determine the stoichiometry of Ly49A–D^d *cis* complexes *in situ*, we exposed C1498 transfectants to the cell impermeable cross-linker *Bis* (Sulfosuccinimidyl)suberate (BS3). Following Ly49A immunoprecipitation (i.p.) and SDS-PAGE under reducing conditions, we detected a predominant band of 80–90 kD (Figure 4A), which corresponds to the Ly49A homodimer (Figure S3A) and an additional band of 140–150 kD, which included both Ly49A (Figure 4A) and D^d (Figure 4B). A corresponding complex of 140–150 kD was observed following D^d i.p. (Figure S4A) but was absent when Ly49A cells did not co-express D^d or in the absence of BS3 treatment (Figure 4A). The molecular weight of 140–150 kD suggests a complex of one Ly49A homodimer (80–90 kD) (Figure S3A) linked to a single D^d heavy chain (45 kD) with or without the β_2m light chain (10 kD) (Figure S4C). Importantly, there was essentially no evidence for Ly49A–D^d complexes of >150 kD, which would be expected if one Ly49A homodimer associated with two D^d molecules (predicted size ~200 kD). We conclude that Ly49A and D^d are constitutively associated on living cells and that *cis* complexes consist of an Ly49A homodimer associated with a single D^d molecule, in agreement with the structural model (Figure 3B).

The stoichiometry of Ly49A–D^d *trans* binding was assessed using soluble Ly49A (Figure 5A). Soluble Ly49A dimers, obtained by fusing the Fc region of human IgG1 to most of the extracellular portion of Ly49A (Figure S5A), specifically bound D^d transfected C1498 cells (Figure 5B). After cross-linking soluble Fc-Ly49A to D^d transfectants and Fc-Ly49A i.p. we detected D^d-containing complexes of ~200 and ~100 kD (Figure 4C). These correspond to complexes of one Fc–Ly49A dimer (~110 kD) (Figure S5A) associated with two D^d molecules (90–110 kD), and of a single Fc–Ly49A chain (~55 kD) (Figure S5A) linked to a single D^d heavy (with or without the β2m light chain (45–55 kD) (Figure S5A). There was essentially no evidence for complexes of ~160 kD, which would be expected if a Fc–Ly49A homodimer (~110 kD) was cross-linked to a single D^d molecule (45–55 kD). These data indicate that

trans binding (by soluble Ly49A dimers) occurred in a bivalent fashion, whereas *cis* binding was monovalent.

Modifications of the Receptor Stalk Dissociate *Cis* from *Trans* binding

The Ly49L-EC structure revealed that the NKDs make numerous contacts with the $\alpha3_S$ helices of the stalk (Figure 2, Table S2), and that many of these interactions are probably conserved across the Ly49 family (see above). If the Ly49L-EC structure indeed represents a *trans*-binding conformation (Figure 3A), disruption of NKD–$\alpha3_S$ interactions should interfere with *trans*, but not *cis*, binding. In addition, the long Ly49 stalk should be essential for *trans* binding, to allow the Ly49 NKDs to fold back onto the stalk, but less critical for *cis* binding, as the NKDs are dissociated from the stalk (Figure 3). To test these predictions, we deleted known and/or predicted α-helical segments (α_S) from the Ly49A stalk (Figure 5A, Figure S2A,B). The resulting Ly49A stalk deletion variants were stably introduced into C1498 (H-2^b) cells, where they were detected using D^d tetramers and Ly49A mAb JR9 (Table 1) or A1 (not shown), which indicated proper folding of the NKDs.

A cell-cell adhesion assay was used to determine whether the Ly49A stalk deletion variants bound membrane-anchored D^d. Wild type Ly49A mediated efficient adhesion to D^d+ cells (>50% conjugates) (Figure 5D, Table 1). This was based on a specific interaction since conjugate formation was inefficient in the absence of Ly49A or D^d or both (~10% conjugates) (Figure 5D, Table 1). Compared to wild type, the deletion of the $\alpha3_S$ segment from the Ly49A stalk ($\Delta\alpha3_S$) significantly reduced adhesion (Table 1). This was not likely due to the reduced length of the stalk, since adhesion was efficient when the $\alpha1_S$ or the $\alpha2_S$ segments were deleted ($\Delta\alpha1_S$ and $\Delta\alpha2_S$) (Table 1). A need for $\alpha3_S$ for *trans* binding was confirmed using soluble Ly49A: While soluble receptors that contained $\alpha3_S$ ($\Delta\alpha1_S$ and $\Delta\alpha1\text{-}2_S$) stained D^d-expressing cells (Figure 5B), there was no binding in the absence of $\alpha3_S$ ($\Delta\alpha1_S$ Δ $\alpha3_S$) (Figure 5B). Importantly, this $\Delta\alpha3_S$ receptor reacted with Ly49A mAb (Figure S5B), indicating that the NKDs were properly folded. We conclude that the $\alpha3_S$ segment plays a role for *trans* binding, consistent with a requirement for back-folding of the NKDs onto $\alpha3_S$.

When the Ly49A stalk was shortened further, by deleting two α-helical segments ($\Delta\alpha1\text{-}2_S$ or $\Delta\alpha_S2\text{-}3_S$), cell-cell adhesion was completely lost (Table 1). However, the soluble version of the $\Delta\alpha1\text{-}2_S$ receptor efficiently stained D^d+ cells (Figure 5B). These data suggest that it the attachment of the $\Delta\alpha1\text{-}2_S$ to a cell membrane precludes ligand binding. This outcome is expected if *trans* recognition is mediated by a receptor conformation in which the NKDs are back-folded onto the stalk. In this case, steric clashes with the cell membrane prevent MHC-I binding.

We next addressed whether *cis* binding showed a corresponding dependence on the length of the stalk and/or on the presence of $\alpha3_S$. Cell-cell adhesion mediated by wild type Ly49A was considerably reduced when Ly49A was co-expressed with D^d (Figure 5D, Table 1). *Cis* D^d masks a large fraction of wild type Ly49A and this prevents *cis*-engaged Ly49A from interacting with D^d in *trans* (Back et al., 2007). Similar to wild type, D^d expression in *cis* reduced adhesion by Ly49A variants, which lacked a single α_S element ($\Delta\alpha1_S$, $\Delta\alpha2_S$ or $\Delta\alpha3_S$) (Table 1), indicating that all these variants bind D^d in *cis*. Corresponding experiments using $\Delta\alpha1\text{-}2_S$ or $\Delta\alpha2\text{-}3_S$ receptors were not informative, as these variants did not mediate specific adhesion.

Cis binding was further tested by comparing D^d tetramer binding to Ly49A before and after disrupting MHC-I complexes (Doucey et al., 2004; Scarpellino et al., 2007). A brief exposure of live cells to an acidic buffer disrupted trimolecular MHC-I complexes, as judged by the complete loss of the β_2m light chain from the cell surface (Figure 5E). Acid treatment of control (H-2^b) transfectants did not alter Ly49A detection using mAb or D^d tetramer (Figure 5E),

suggesting that Ly49A is not acid-sensitive and is not significantly masked by K^b or D^b molecules. Co-expression of Ly49A and D^d significantly reduced D^d tetramer binding and this was reversed by acid treatment (Figure 5E, Table 1) (Doucey et al., 2004; Scarpellino et al., 2007). Likewise, acid stripping considerably improved D^d tetramer binding to all Ly49A receptor variants lacking a single α-helical stalk segment (Table 1). Acid treatment also increased tetramer binding to Ly49A $\Delta\alpha1\text{-}2_S$ and $\Delta\alpha2\text{-}3_S$ receptors (Table 1), indicating that very short Ly49A variants were masked by *cis* D^d. The physical association of D^d with Ly49A variants lacking one, and even two, α_S elements was confirmed using co-i.p. (Figure 5F and data not shown). Thus, very short Ly49A variants, which retain a single α_S segment, can bind D^d expressed in *cis* but not *in trans*. This outcome is expected if *trans* binding requires back-folded and *cis* binding extended Ly49 conformations, respectively (Figure 3). Consistent with this interpretation, $\alpha3_S$ is not essential for *cis* binding suggesting that back-folding of the NKD is not required for *cis* interaction.

The Loop Region between the Stalk and the NKD Is Essential for *Cis* Binding

A prominent feature of the Ly49L-EC structure is the 12-residue L_S loop, which links $\alpha3_S$ to the NKD (Figure 2). This apparently flexible loop may allow the NKD to back-fold onto the stalk for *trans* binding to MHC-I (Figure 3A) or it may be needed for the NKD to assume an extended conformation for *cis* binding (Figure 3B) or it may contribute to both *trans* and *cis* interactions. To distinguish among these possibilities, we deleted the L_S loop (aa 128–137; ΔL_S) (Figure S2B) from full-length Ly49A. The ΔL_S receptor mediated efficient conjugation with D^d+ cells (Table 1) and a soluble version of this receptor efficiently stained D^d+ cells (Figure 5C), indicating that the L_S loop is not essential for *trans* binding. Based on the Ly49L-EC structure, the α-carbons of Thr127 and Gly138 are estimated to be 9.5 Å apart in wild type Ly49A. This distance should allow Thr127 and Gly138 to be connected in the ΔL_S mutant through minor structural adjustments of residues Gly138–Lys140, without disturbing the back-folded conformation. While *trans* binding was intact, the ΔL_S receptor failed to bind D^d in *cis* (Table 1). These data suggest that L_S allows Ly49A to adopt an extended conformation needed to engage MHC-I on the same cell.

To determine whether the role of L_S is mediated by a specific amino acid sequence, we replaced the wild type loop with a glycine-rich sequence (G-L_S) of equal length (Figure S3B), which should confer a high degree of flexibility to the NKDs. In contrast to removal of the loop, its replacement diminished adhesion to D^d+ cells (Table 1). In addition, staining of D^d+ cells using a soluble version of the G-L_S receptor was very inefficient (Figure 5C), although the fusion protein reacted with Ly49A mAb (Figure S5C,D), implying proper folding of the NKDs. Even though the deletion of L_S was compatible with *trans* binding, its replacement interfered with *trans* binding. This indicated that *trans* binding requires a specific amino acid sequence. Despite impaired *trans* binding, the G-L_S variant showed a significant, albeit limited, ability to bind D^d in *cis* (Table 1). Therefore, a glycine-rich loop can rescue ΔL_S with respect to *cis* binding, indicating that the L_S loop needs to provide spacing and/or flexibility to allow *cis* binding. Overall, the data show that the L_S loop region is essential for *cis* but not for *trans* binding.

Dissociation of Ly49A *Trans* Binding from Inhibitory Receptor Function

Our mutational analyses identified elements of the Ly49A stalk, notably α_S1, α_S2 and L_S, that were not required for Ly49A–D^d *trans* binding. To address whether these elements were needed for receptor function, we introduced the respective stalk deletion mutants into the rat NK cell line RNK (Figure 6A). RNK lines produced IFNγ upon stimulation with CD161 (NKRP1) mAb (Figure S6). Co-crosslinking of CD161 and Ly49A (using mAb A1, which binds the Ly49A NKD) inhibited IFNγ production by RNK cells expressing wild type Ly49A as well as

those expressing stalk mutant receptors (Figure S6). This demonstrated that the mutant receptors are competent to transduce inhibitory signals.

Next we tested function of mutant Ly49A receptors using cellular targets. Parental RNK cells killed untransfected and D^d+ YB2/0 target cells (Figure 6B). Introduction of wild type Ly49A into RNK cells strongly inhibited lysis of D^d+ targets (Figure 6B), as shown previously (Nakamura et al., 1997). As expected, lysis inhibition was not observed with the very short Ly49A stalk variants $\Delta\alpha_S$1-2 (not shown) or $\Delta\alpha_S$2-3 (Figure 6B), which did not bind D^d in *trans* (Table 1). Unexpectedly, lysis inhibition was also not observed when a single α-helical segment was deleted from the Ly49A stalk ($\Delta\alpha_S$1 or $\Delta\alpha_S$2) (Figure 6B,D), despite the fact that such variants mediated efficient adhesion to D^d+ cells (Table 1) and that $\Delta\alpha_S$1 was signaling competent (Figure S6). To determine whether deficient function was due to a reduced length of the stalk or some other role of $\alpha1_S$ and/or $\alpha2_S$, we replaced $\alpha1_S$ with sequence from $\alpha2_S$ ($\alpha1_S$ -> $\alpha2_S$). We also replaced the $\alpha1\text{-}2_S$ region with heterologous sequence from the CD72 stalk which, like the Ly49A stalk, is predicted to be α-helical ($\alpha1\text{-}2_S$ -> CD72) (Figure S2B). Both replacements resulted in efficient lysis inhibition (Figure 6C,D). Corresponding results were obtained with RMA target cells expressing the NKG2D ligand H60 (**not shown**). We conclude that an optimal length of the stalk, and not some other function of the $\alpha1_S$ or $\alpha2_S$ segments, is crucial for lysis inhibition by Ly49A.

We also tested lysis inhibition by loop region modified Ly49A variants. The G-L_S receptor did not inhibit lysis (Figure 6B), which was expected based on its reduced *trans* binding capacity (Table 1). Unexpectedly, the ΔL_S variant did also not inhibit lysis (Figure 6B). Despite the fact that the L_S loop is not required for MHC-I binding (Table 1) or inhibitory signaling (Figure S6), it is essential for the inhibitory function of Ly49A.

Redistribution of Ly49A Variants to the Immunological Synapse

To further address the basis for defective function of certain stalk modified receptors, we investigated the redistribution of Ly49A to the immunological synapse, which correlates with inhibitory function (Back et al., 2007). Like synapses formed by primary NK cells (Back et al., 2007), wild type Ly49A accumulated at the site of contact between RNK and D^d-transfected but not untransfected target cells (Figure 6E). Even though the inhibitory capacity of the $\Delta\alpha_S$1 and $\Delta\alpha_S$1 receptors was impaired (Figure 6B,D), they redistributed efficiently to the immune synapse (Figure 6E). Conversely, we did not observe an obvious accumulation of the ΔL_S receptor at the NK cell synapse (Figure 6E), which is in agreement with the deficient inhibitory function of this mutant (Figure 6B). Notwithstanding the adhesive function of this variant (Table 1), low amounts of ΔL_S receptor were detectable at the contact zone (Figure 6E). Corresponding data were obtained when inspecting cellular interfaces between Ly49A and D^d transfected C1498 cells (**not shown**). Staining for an epitope tag present in the intracellular portion ruled out the possibility that ΔL_S was somehow inaccessible to Ly49A mAb at the cellular interface (**not shown**). The L_S loop is thus essential for post-ligand binding events, which allow the redistribution of receptor-ligand complexes to the NK cell synapse and mediate inhibitory receptor function.

Discussion

Due to technical difficulties associated with crystallizing cell surface receptors bearing long stalks (e.g. CD8), X-ray crystallographic studies of such receptors have largely been restricted to their globular ligand binding domains. However, there is increasing evidence that stalk regions may have specialized roles in receptor function, besides simply connecting the ligand binding domains to the membrane. One striking example is the stalk region of the T cell co-receptor CD8, which undergoes developmentally programmed *O*-glycan modification (Moody et al., 2001). Decreased glycosylation of the CD8 stalk during thymic development is associated

with increased affinity for MHC-I and improved T cell signaling, thereby affecting T cell selection. However, the basis for differential binding is not understood, as no three-dimensional structural information is available for the CD8 stalk. Likewise, the structural basis for *cis* versus *trans* recognition of MHC-I by inhibitory immunoreceptors such as Ly49s was unknown prior to this study (Held and Mariuzza, 2008).

Here we provide structural, biochemical and functional evidence that *cis–trans* interactions of Ly49 NK cell receptors with MHC-I are mediated by two distinct receptor conformations. Based on the Ly49L-EC structure, we proposed that NKDs must back-fold onto the $\alpha3_S$ region of the stalk to mediate *trans* interaction. This model was validated in several independent ways, including deletion of the entire $\alpha3_S$ segment from the Ly49A stalk. This resulted in greatly reduced *trans* binding of D^d by the $\Delta\alpha3_S$ variant in a cell-cell adhesion assay, an effect that was not observed when the $\alpha1_S$ or $\alpha2_S$ segment was removed. In addition, *trans* binding by membrane-anchored (but not soluble) Ly49A required the presence of at least two α_S segments, in agreement with our structural model in which steric clashes with the NK cell membrane would preclude *trans* binding of MHC-I to a back-folded receptor lacking $\alpha1_S$ and $\alpha2_S$ (Figure 3A). We further showed that (soluble) Ly49A could bind two membrane-bound D^d molecules in *trans*, as predicted by the model. These findings indicate that *trans* binding is mediated by a receptor conformation in which the NKDs are back-folded onto the stalk. This model also explains early domain swap experiments, which indicated that the specificity of Ly49C was altered when the C-terminal part of its stalk was replaced with that of Ly49A (Brennan et al., 1996). We propose that the predominant (or default) conformation of Ly49 receptors in the absence of *cis* MHC-I is back-folded, since Ly49A on NK cells from H-2^b mice efficiently binds D^d in *trans* and strongly inhibits effector function (Doucey et al., 2004; Karlhofer et al., 1992).

According to our structural model for *cis–trans* interactions, *cis* binding of MHC-I requires Ly49 to assume an extended conformation in which the α3 segments of the stalk do not contact the NKDs (Figure 3B). Indeed, we showed that $\alpha3_S$, which is essential for binding in *trans*, was not required for binding in *cis*, providing evidence that the NKDs are disengaged from the stalk during *cis* interactions. Further, when the stalk region was progressively shortened, *trans* binding was impaired before *cis* binding, as expected if *cis* binding is mediated by an extended receptor. Moreover, we showed that, on living cells, the Ly49A–D^d *cis* complex consists of an Ly49A homodimer associated with a single D^d molecule, as predicted by the model (Figure 3B). Collectively, these results provide strong experimental evidence that *cis* and *trans* interactions are mediated by extended and back-folded conformations, respectively, of the Ly49 receptor.

Mutational analysis of the flexible L_S loop, which links $\alpha3_S$ to the NKD, produced insights into Ly49 function beyond those predicted by the structural model. Although deletion of L_S did not interfere with *trans* binding, the loop was required for *cis* binding, most likely by permitting Ly49 to switch from the back-folded to extended conformation. This particular function of L_S was sequence-independent, since the loop could be replaced by a glycine-rich sequence. Unexpectedly, even though the L_S loop was not needed for MHC-I binding in *trans* or the transduction of inhibition signals, L_S was nevertheless essential for lysis inhibition. Typically, the engagement of cell surface receptors induces intracellular signaling via two principle mechanisms: ligand-induced structural changes in the receptor and/or oligomerization of receptor–ligand complexes (Schwartz et al., 2002). We previously showed that Ly49C in complex with H-$2K^b$ retains nearly the same structure as the free receptor (Deng et al., 2008), arguing against MHC-induced conformational changes in Ly49 as a signaling mechanism. On the other hand, zinc-dependent multimerization of KIR is thought to promote the formation of clusters of KIR and HLA-C molecules at the NK cell immune synapse, resulting in inhibitory function (Boyington et al., 2000). Similarly, Ly49 signaling may depend

on clustering of ligand-engaged Ly49 dimers. Although it is not immediately obvious how lateral association of Ly49–MHC-I complexes might occur, our data suggest that L_S could contribute to clustering, since the loop deficient receptor failed to accumulate at the immune synapse. In the modeled bivalent Ly49–MHC-I *trans* complex (Figure 3A), the L_S loop is on the exterior of the complex, fully exposed to solvent, such that it could potentially mediate lateral interactions with other cell surface molecules or adjacent bivalent Ly49–MHC-I *trans* complexes. A analogous ligand-induced, receptor-mediated lateral association is essential for the activation of the epidermal growth factor receptor (EGFR) (Ogiso et al., 2002).

The analysis of receptors lacking a single α_S segment ($\Delta\alpha1_S$ and $\Delta\alpha2_S$) revealed an additional discrepancy between ligand binding and inhibitory receptor function. In contrast to deletion of the L_S loop, receptors with a shortened stalk did accumulate efficiently at the immune synapse. Lysis inhibition was restored when the $\alpha1_S$ or the entire $\alpha1\text{-}2_S$ region was replaced with a heterologous stalk. This demonstrated that a minimal length of the stalk, and not some other function of the $\alpha1_S$ or $\alpha2_S$ segments, was critical for inhibitory Ly49 receptor function. It is thought that inhibitory receptors must be co-engaged with activating NK cell receptors in submicroscopic clusters in order to antagonize activation signaling (Treanor et al., 2006). According to the concept of size-based segregation of cell surface molecules (Choudhuri et al., 2005; Velikovsky et al., 2007), activating and inhibitory receptor–ligand pairs should fit into the narrow synaptic cleft of 100–150 Å between the NK cell and the target cell membrane. Activating and inhibitory interactions may thus become mutually exclusive when the Ly49 stalk is too short. For example, when the activating NKG2D receptor engages its H60 ligand (which was the case when RNK cells were used against RMA H60 targets), the shortened inhibitory receptor may be unable to reach across to D^d molecules on target cells. Consequently, lysis would not be inhibited. Conversely, when the shortened inhibitory receptor interacts with ligand (consistent with physical interaction), the activating receptor–ligand pair may not fit into the narrowed synaptic cleft between the two juxtaposed membranes. Such a microcluster would not contribute to activation signaling.

We propose that other receptors acting in both *cis* and *trans* undergo large structural rearrangements analogous to those of Ly49. Similar to Ly49, *cis–trans* binding by LILRB2 and PIR-B receptors shows broad MHC-I specificity (Masuda et al., 2007) and is thus likely mediated by the same binding site. If so, the ligand binding D1 and D2 domains of LILRB2 would need to reverse direction with respect to the effector cell surface to bind MHC-I in *cis*. This would require that LILRB2 bends back on itself and adopts a horseshoe-shaped configuration of the four Ig domains (D1–D4). Such a large reversal implies considerable flexibility in the segment connecting the D2 with the D3 domain. Consistent with this possibility, the four N-terminal Ig-like domains of the *Drosophila* Dscam protein indeed assume a horseshoe arrangement, which is made possible by a five-residue hinge between D2 and D3 (Meijers et al., 2007). In the case of PIB-B, which has two additional membrane proximal Ig-like domains compared to LILRB2, the D4–D5 or D5–D6 connecting segments might provide further flexibility. Therefore, the ability to reverse orientation may be a general feature of receptors binding in *cis* and *trans*, involving at least two structurally distinct strategies: exceptionally long stalk regions in the case of Ly49s and very flexible, or multiple, interdomain hinges in the case of LILRB2 and PIR-B.

In summary, based on crystal structure determinations, mutational analysis and functional assays, we have shown that the Ly49 stalk region mediates several essential functions. First, the stalk allows Ly49 receptors to reorient their NKDs relative to the NK cell membrane in order to engage MHC-I in *trans* (back-folded conformation) or *cis* (extended conformation). Second, the stalk provides sufficient distance between the NKDs and the NK cell membrane for *trans* binding of MHC-I, which requires a minimum of two α_S segments. Third, the stalk permits optimal spacing between the NK cell and target cell membranes for productive Ly49–

MHC-I interactions at the immune synapse, which requires all three α_S segments. Fourth, the L_S loop is essential for efficient accumulation of Ly49–MHC-I complexes at the NK cell synapse, which is necessary for inhibitory function. Together, these results demonstrate that stalk regions can have multiple specialized roles in receptor function, well beyond simply attaching the ligand-binding domains to the cell membrane.

Experimental Procedures

Protein Expression, Purification, Crystallization and Structure Determination

The extracellular portion of Ly49L from mouse strain C3H (Ly49L-EC; residues 79–265), comprising the NKD and most of the stalk region, was cloned into the vector pT7-7 (Novagen). The protein was expressed in *Escherichia coli* as inclusion bodies, solubilized in 6 M guanidine, and folded *in vitro* by dilution into 30% (volume/volume) glycerol, 0.4 M arginine, 3 mM reduced glutathione, and 0.8 mM oxidized glutathione. Ly49L was purified with sequential MonoS and Superdex 75 HR columns (Amersham Biosciences). The NKD of Ly49L (residues 138–265) was prepared similarly. Details on crystallization, data collection, structure determination, and secondary structure predictions are provided in Supplemental Experimental Procedures.

Flow Cytometry

The Ly49A stalk variants described herein (Figure S2B) were generated and expressed using procedures described in the Supplementary Methods. Acid treatment of stable transfectants (Doucey et al., 2004) and cell-cell adhesion assays (Back et al., 2007) were described before.

Cells were surface stained with mAbs to H-2D^d (34-2-12), Ly49A (JR9-318) or β_2m (Ly-m11) (BD Pharmingen). Binding of soluble Fc–Ly49A fusion proteins was revealed using PE-conjugated anti-human IgG (Jackson Lab). D^d-HIV-mouse β_2m tetramers were produced as described before (Scarpellino et al., 2007). Three-color flow cytometry was performed using a FACScan flow cytometer (Becton Dickinson) and Flowjow (Tree Star, Ashland, OR) software for data evaluation.

Chemical Cross-linking

C1498 transfectants (10^7) were incubated for 30 min with 0.25 mM of BS3 (Bis (Sulfosuccinimidyl) suberate (BS3) (Pierce)) in 1 ml of PBS at 4 °C. In some experiments, D^d transfectants cells were reacted with soluble Fc–Ly49A (2 μg/10^7 cells) prior to cross-linking using decreasing concentrations of BS3 (0.25, 0.05 and 0.01 mM). Excess cross-linker was quenched by washes in TBS. The cells were lysed at 4 °C in Tris buffer (50 mM Tris pH 7.5, 150 mM NaCl, 1% NP40) and lysates were immunoprecipitated using VSV-agarose or Protein G Sepharose (Sigma). Immunoprecipitates were separated using reducing SDS-PAGE, transferred to nitrocellulose membranes and analysed using anti-HA (3F10, Roche) or anti-VSV (P5D4, Sigma) Western blot as described (Doucey et al., 2004).

Confocal Microscopy

RNK cells expressing Ly49A were mixed with YB2/0 D^d-YFP cells at a 1:1 ratio, centrifuged and incubated for 8–10 min at 37 °C. After resuspending, conjugates were adhered for 1–2 min to poly-L or poly-D lysine coated slides before fixation for 10 min using cold acetone. Ly49A was stained using mAb JR9-318 followed by Alexa 568-conjugated goat-anti mouse IgG Ab (Molecular Probes). Confocal microscopy and image quantification have been described before (Back et al., 2007).

Statistical Analysis

All p values were determined using a two-tailed student's t-test with equal sample variance. Data sets were considered significantly different when $p<0.05$.

Accession Codes

Coordinates and structure factors for Ly49L NKD and Ly49L-EC have been deposited in the Protein Data Bank under accession codes 3G8K and 3G8L, respectively.

Supplementary Material

Refer to Web version on PubMed Central for supplementary material.

Acknowledgments

This work was supported in part by grants from the Swiss National Science Foundation and Oncosuisse to W.H. and by the National Institutes of Health (AI47990 to R.A.M.). E.L.M. is supported by the Fogarty International Center (TW007972). We are grateful to P. Guillaume (Ludwig Institute) for tetramers, F. Lévy (Ludwig Institute) for MHC-I Abs, S.K. Anderson (National Cancer Institute) and A.P. Makrigiannis (Clinical Research Institute of Montreal) for Ly49L cDNA, and Howard Robinson (Brookhaven National Synchrotron Light Source) for X-ray data collection.

References

Anfossi N, Andre P, Guia S, Falk CS, Roetynck S, Stewart CA, Breso V, Frassati C, Reviron D, Middleton D, et al. Human NK cell education by inhibitory receptors for MHC class I. Immunity 2006;25:331–342. [PubMed: 16901727]

Back J, Chalifour A, Scarpellino L, Held W. Stable masking by H-2Dd cis ligand limits Ly49A relocalization to the site of NK cell/target cell contact. Proc Natl Acad Sci USA 2007;104:3978–3983. [PubMed: 17360463]

Boyington JC, Motyka SA, Schuck P, Brooks AG, Sun PD. Crystal structure of an NK cell immunoglobulin-like receptor in complex with its class I MHC ligand. Nature 2000;405:537–543. [PubMed: 10850706]

Brennan J, Mahon G, Mager DL, Jefferies WA, Takei F. Recognition of class I major histocompatibility complex molecules by Ly49: Specificities and domain interactions. J Exp Med 1996;183:1553–1559. [PubMed: 8666913]

Burshtyn D, Scharenberg A, Wagtmann N, Rajagopalan S, Peruzzi M, Kinet JP, Long EO. Recruitment of tyrosine phosphatase HCP by the NK cell inhibitory receptor. Immunity 1996;4:77–85. [PubMed: 8574854]

Chalifour A, Scarpellino L, Back J, Brodin P, Devèvre E, Gros F, Lévy F, Leclercq G, Höglund P, Beermann F, Held W. A role for *cis* interaction between the inhibitory Ly49A receptor and MHC class I for natural killer cell education. Immunity 2009;30:337–347. [PubMed: 19249231]

Choudhuri K, Wiseman D, Brown MH, Gould K, van der Merwe PA. T-cell receptor triggering is critically dependent on the dimensions of its peptide-MHC ligand. Nature 2005;436:578–582. [PubMed: 16049493]

Dam J, Baber J, Grishaev A, Malchiodi EL, Schuck P, Bax A, Mariuzza RA. Variable dimerization of the Ly49A natural killer cell receptor results in differential engagement of its MHC class I ligand. J Mol Biol 2006;362:102–113. [PubMed: 16899255]

Dam J, Guan R, Natarajan K, Dimasi N, Chlewicki LK, Kranz DM, Schuck P, Margulies DH, Mariuzza RA. Variable MHC class I engagement by Ly49 natiral killer cell receptors demonstrated by the crystal structure of Ly49C bound to H-2K^b. Nat Immunol 2003;4:1213–1222. [PubMed: 14595439]

Deng L, Cho S, Malchiodi EL, Kerzic MC, Dam J, Mariuzza RA. Molecular architecture of the MHC-binding site of Ly49 natural killer cell receptors. J Biol Chem 2008;283:16840–16849. [PubMed: 18426793]

Deng L, Mariuzza RA. Structural basis for recognition of MHC and MHC-like ligands by natural killer cell receptors. Semin Immunol 2006;18:159–166. [PubMed: 16737824]

Doucey MA, Scarpellino L, Zimmer J, Guillaume P, Luescher IF, Bron C, Held W. *Cis*-association of Ly49A with MHC class I restricts natural killer cell inhibition. Nat Immunol 2004;5:328–336. [PubMed: 14973437]

Fernandez NC, Treiner E, Vance RE, Jamieson AM, Lemieux S, Raulet DH. A subset of natural killer cells achieve self-tolerance without expressing inhibitory receptors specific for self MHC molecules. Blood 2005;105:4416–4423. [PubMed: 15728129]

Held W, Mariuzza RA. *Cis* interactions of immunoreceptors with MHC and non-MHC ligands. Nat Rev Immunol 2008;8:269–278. [PubMed: 18309314]

Karlhofer FM, Ribaudo RK, Yokoyama WM. MHC class I alloantigen specificity of Ly-49+ IL-2 activated natural killer cells. Nature 1992;358:66–70. [PubMed: 1614533]

Kim S, Poursine-Laurent J, Truscott SM, Lybarger L, Song YJ, Yang L, French AR, Sunwoo JB, Lemieux S, Hansen TH, Yokoyama WM. Licensing of natural killer cells by host major histocompatibility complex class I molecules. Nature 2005;436:709–713. [PubMed: 16079848]

Lanier LL. NK cell recognition. Annu Rev Immunol 2005;23:225–274. [PubMed: 15771571]

Masuda A, Nakamura A, Maeda T, Sakamoto Y, Takai T. Cis binding between inhibitory receptors and MHC class I can regulate mast cell activation. J Exp Med 2007;204:907–920. [PubMed: 17420263]

Meijers R, Puettmann-Holgado R, Skiniotis G, Liu JH, Walz T, Wang JH, Schmucker D. Structural basis of Dscam isoform specificity. Nature 2007;449:487–491. [PubMed: 17721508]

Moody AM, Chui D, Reche PA, Priatel JJ, Marth JD, Reinherz EL. Developmentally regulated glycosylation of the CD8αβ coreceptor stalk modulates ligand binding. Cell 2001;107:501–512. [PubMed: 11719190]

Nakamura MC, Niemi EC, Fisher MJ, Shultz LD, Seaman WE, Ryan JC. Mouse Ly-49A interrupts early signaling events in NK cell cytotoxicity and functionally associates with the SHP-1 tyrosine phosphatase. J Exp Med 1997;185:673–684. [PubMed: 9034146]

Natarajan K, Dimasi N, Wang J, Mariuzza RA, Margulies DH. Structure and function of natural killer cell receptors: Multiple solutions to self, nonself discrimination. Annu Rev Immunol 2002;20:853–885. [PubMed: 11861620]

Ogiso H, Ishitani R, Nureki O, Fukai S, Yamanaka M, Kim JH, Saito K, Sakamoto A, Inoue M, Shirouzu M, Yokoyama S. Crystal structure of the complex of human epidermal growth factor and receptor extracellular domains. Cell 2002;110:775–787. [PubMed: 12297050]

Peterson ME, Long EO. Inhibitory receptor signaling via tyrosine phosphorylation of the adaptor Crk. Immunity 2008;29:578–588. [PubMed: 18835194]

Scarpellino L, Oeschger F, Guillaume P, Coudert JD, Levy F, Leclercq G, Held W. Interactions of Ly49 family receptors with MHC class I ligands in *trans* and *cis*. J Immunol 2007;178:1277–1284. [PubMed: 17237373]

Schwartz JC, Zhang X, Nathenson SG, Almo SC. Structural mechanisms of costimulation. Nat Immunol 2002;3:427–434. [PubMed: 11976720]

Tormo J, Natarajan K, Margulies DH, Mariuzza RA. Crystal structure of a lectin-like natural killer cell receptor bound to its MHC class I ligand. Nature 1999;402:623–631. [PubMed: 10604468]

Treanor B, Lanigan PM, Kumar S, Dunsby C, Munro I, Auksorius E, Culley FJ, Purbhoo MA, Phillips D, Neil MA, et al. Microclusters of inhibitory killer immunoglobulin-like receptor signaling at natural killer cell immunological synapses. J Cell Biol 2006;174:153–161. [PubMed: 16801390]

Velikovsky CA, Deng L, Chlewicki LK, Fernandez MM, Kumar V, Mariuzza RA. Structure of natural killer receptor 2B4 bound to CD48 reveals basis for heterophilic recognition in signaling lymphocyte activation molecule family. Immunity 2007;27:572–584. [PubMed: 17950006]

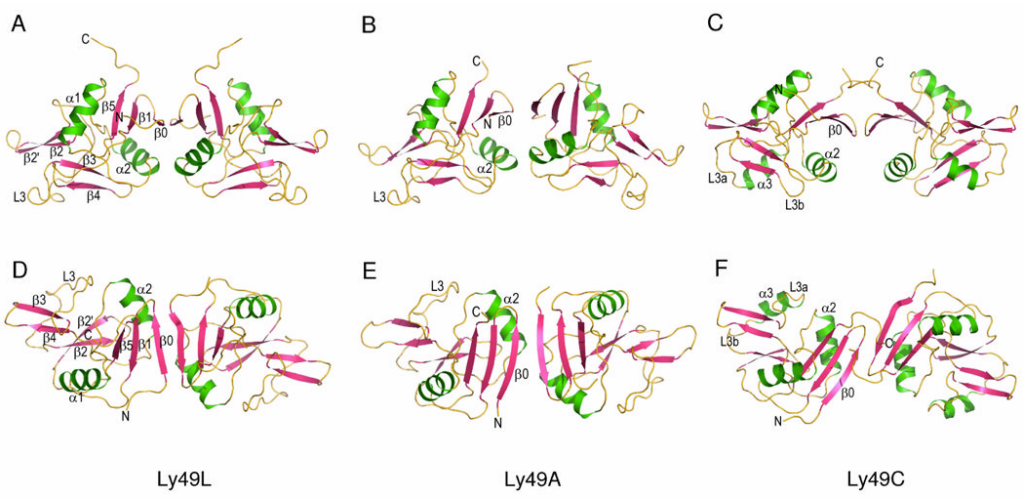

Figure 1.

Variability in Dimerization Mode of Ly49 Receptors. (**A-C**) Side views of the Ly49L, Ly49A (PDB accession code 1QO3) and Ly49C (3C8J) NKD homodimers (ribbon diagrams). All three Ly49 structures lack stalk regions. Secondary structure elements are labeled; α-helices are green, β-strands are pink and loops are yellow. Ly49C contains a third α-helix (α3) not found in Ly49L or Ly49A. The N- and C-termini are indicated. (**D-F**) Top views of the Ly49L, Ly49A and Ly49C dimers.

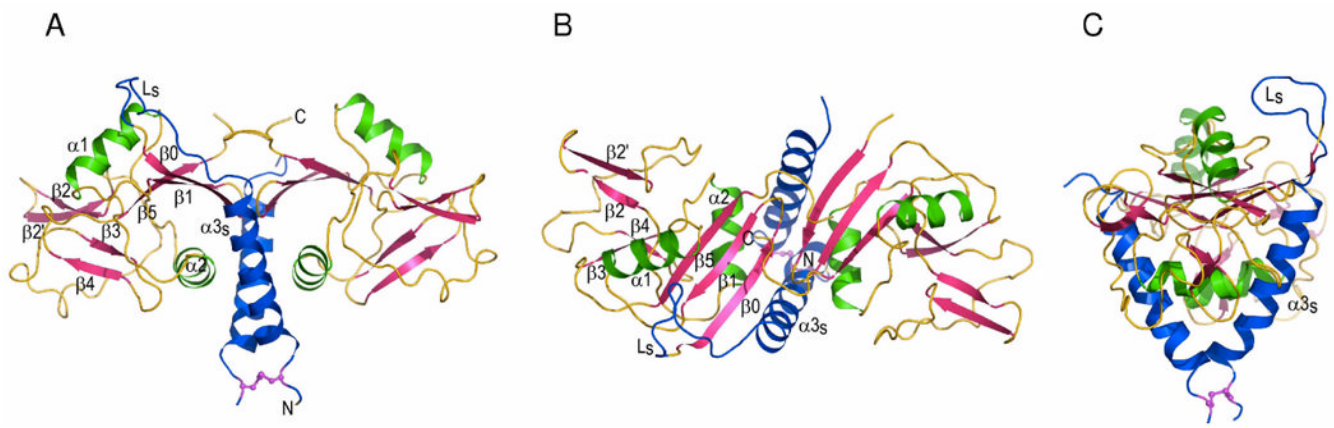

Figure 2.

Structure of Ly49L with Stalk Region. (**A**) Side view of the Ly49L-EC homodimer. The orientation is the same as in Figure 1A. The stalk (blue) is composed of helix $\alpha 3_S$ and loop L_S. Most of L_S is disordered in the right-hand monomer of the Ly49L dimer. The N-terminal Cys110–Cys110 disulfide bond is magenta. (**B**) Top view of Ly49L-EC. The orientation is the same as in Figure 1D. (**C**) Ly49L-EC rotated 90° clockwise with respect to the view in (**A**).

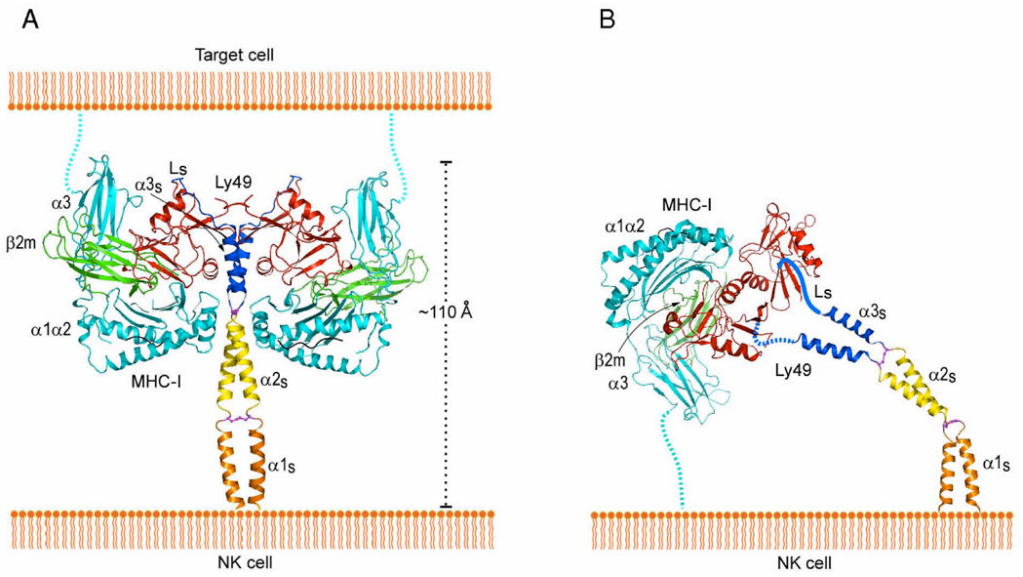

Figure 3.

Hypothetical Model for *Trans* and *Cis* Interactions of Ly49 Receptors with MHC-I Ligands. (**A**) *Trans* interaction of an Ly49 receptor with two MHC-I molecules, based on the structures of Ly49L-EC and the Ly49C–H-2K^b complex (PDB accession code 3C8K). The α1, α2 and α3 domains of the MHC-I heavy chain are cyan; β_2m is green; Ly49 NKD is red; helix $\alpha3_S$ of the Ly49 stalk and loop L_S connecting $\alpha3_S$ to the NKD are blue; the disulfide bond linking the $\alpha3_S$ helices is magenta. The predicted $\alpha1_S$ and $\alpha2_S$ helices of the stalk are drawn arbitrarily in orange and yellow, respectively, with the putative disulfide bond in magenta. The Ly49 homodimer on the NK cell binds two MHC-I molecules on the target cell. To bind in *trans*, the stalks must adopt a back-folded conformation, as the N-termini of the Ly49 monomers point away from the NK cell membrane (Ly49s are type II transmembrane proteins). (**B**) *Cis* interaction of Ly49 with MHC-I, based on the structure of Ly49L-EC and the Ly49A–H-2D^d complex (1QO3). The L_S loops connecting the $\alpha3_S$ helices to the NKDs are drawn arbitrarily. The Ly49 homodimer binds one MHC-I molecule on the NK cell itself. In this case, the stalks must assume an extended conformation, as the N-termini of the Ly49 monomers point towards the NK cell. Adapted and updated from (Held and Mariuzza, 2008).

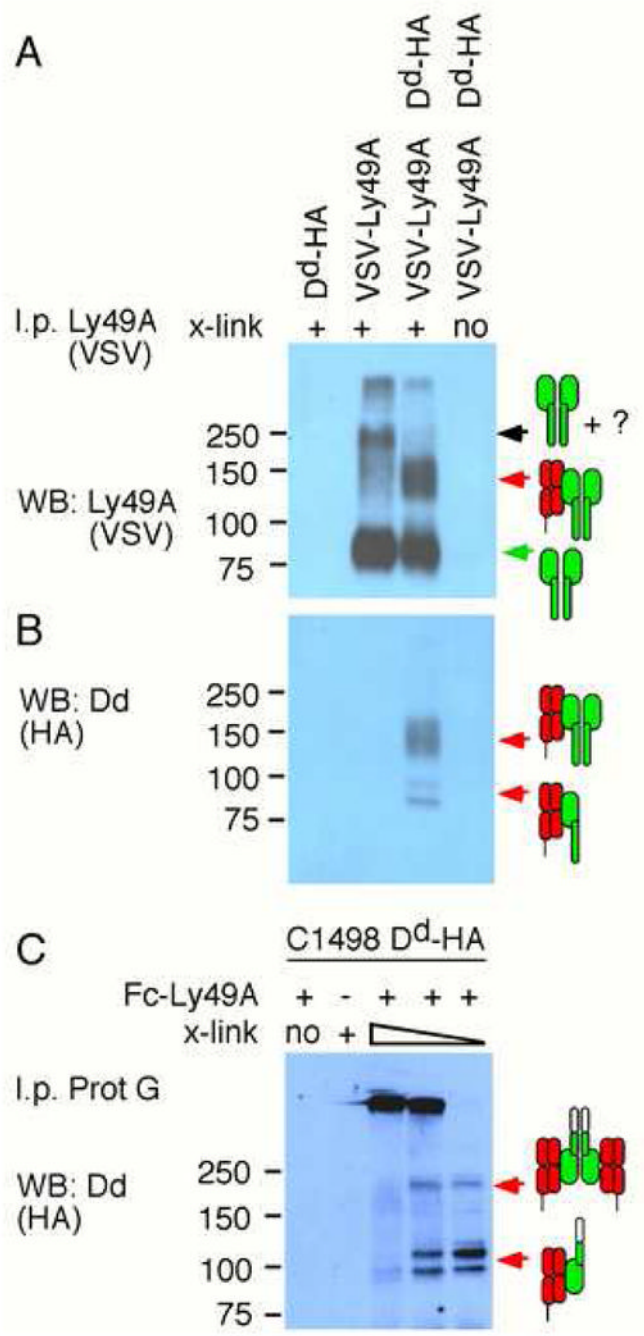

Figure 4.

Stoichiometry of Ly49A–D^d *Cis* and *Trans* Complexes. Stable transfectants expressing D^d and/or Ly49A were exposed to the chemical cross-linker BS3. The Ly49A immunoprecipitate (i.p.) was analyzed by reducing SDS-PAGE and western blotting (WB) specific for Ly49A (VSV tag) (**A**) and for D^d (HA tag) (**B**). (**C**) Soluble Fc–Ly49A receptor was reacted with D^d transfectants prior to covalent cross-linking. Protein G i.p. was analyzed by WB for D^d(-HA).

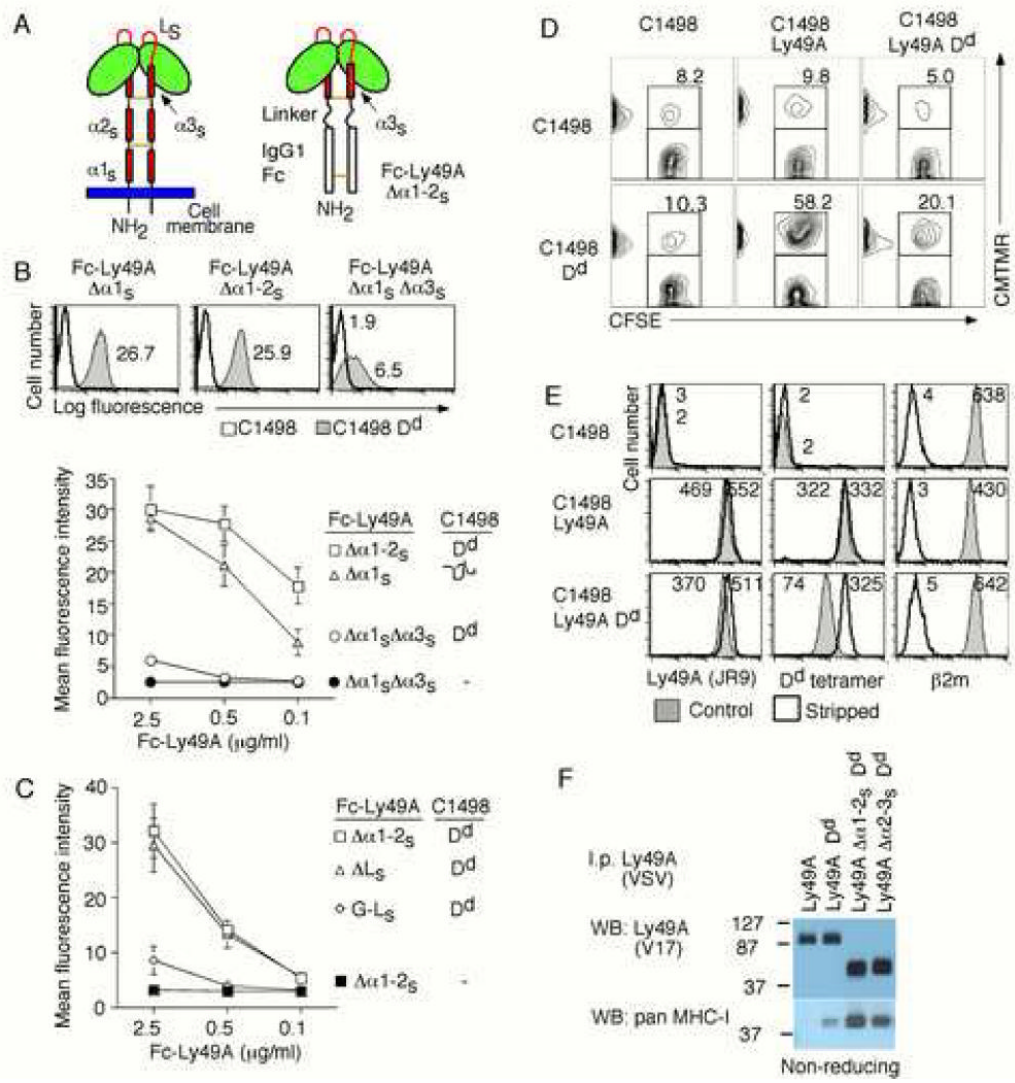

Figure 5.

Cis and *Trans* Binding by Stalk Modified Ly49A Receptors. (**A**) The two Ly49A subunits comprise a ligand binding domain (green), which is connected by a loop (L_S) and known ($\alpha3_S$) and predicted ($\alpha2_S$ and $\alpha1_S$) α-helical segments to the NK cell membrane. Soluble Fc-Ly49A dimers consist of the human IgG1 Fc region fused to Ly49A. (**B**) D^d+ (grey histogram) and non-transfected C1498 cells (open histogram) were stained with soluble Fc-Ly49A (2.5 μg/ml) corresponding to the $\Delta\alpha1\text{-}2_S$ or the $\Delta\alpha1_S$ receptor, which contained or lacked $\alpha3_S$. Numbers indicate the mean fluorescence intensity (MFI) of staining. The line graph depicts the MFI of staining in relation to the Fc–Ly49 concentration (**C**) As in (**B**) except that the fusion proteins corresponded to the $\Delta\alpha1\text{-}2_S$ receptor, in which the L_S loop was deleted (ΔL_S) or replaced with a glycine-rich sequence (G-L_S). (**D**) C1498 cells expressing Ly49A or D^d were labeled with CMTMR and CFSE, respectively, allowed to adhere, fixed and analysed by flow cytometry. Numbers in the density plots indicate CMTMR+ cells conjugated with CFSE+ cells as a percentage of all CMTMR+ cells. (**E**) C1498 cells expressing Ly49A and/or D^d were exposed to an acidic buffer to disrupt MHC-I-peptide complexes prior to staining with Ly49A mAb (JR9), D^d tetramer or with β_2m mAb. Filled histograms depict the staining before (control) and open histograms after acid treatment (stripped). Numbers indicate the MFIs of staining.

(**F**) The indicated Ly49A immunoprecipitates were analyzed using non-reducing SDS-PAGE and Western blot (WB) specific for MHC-I molecules.

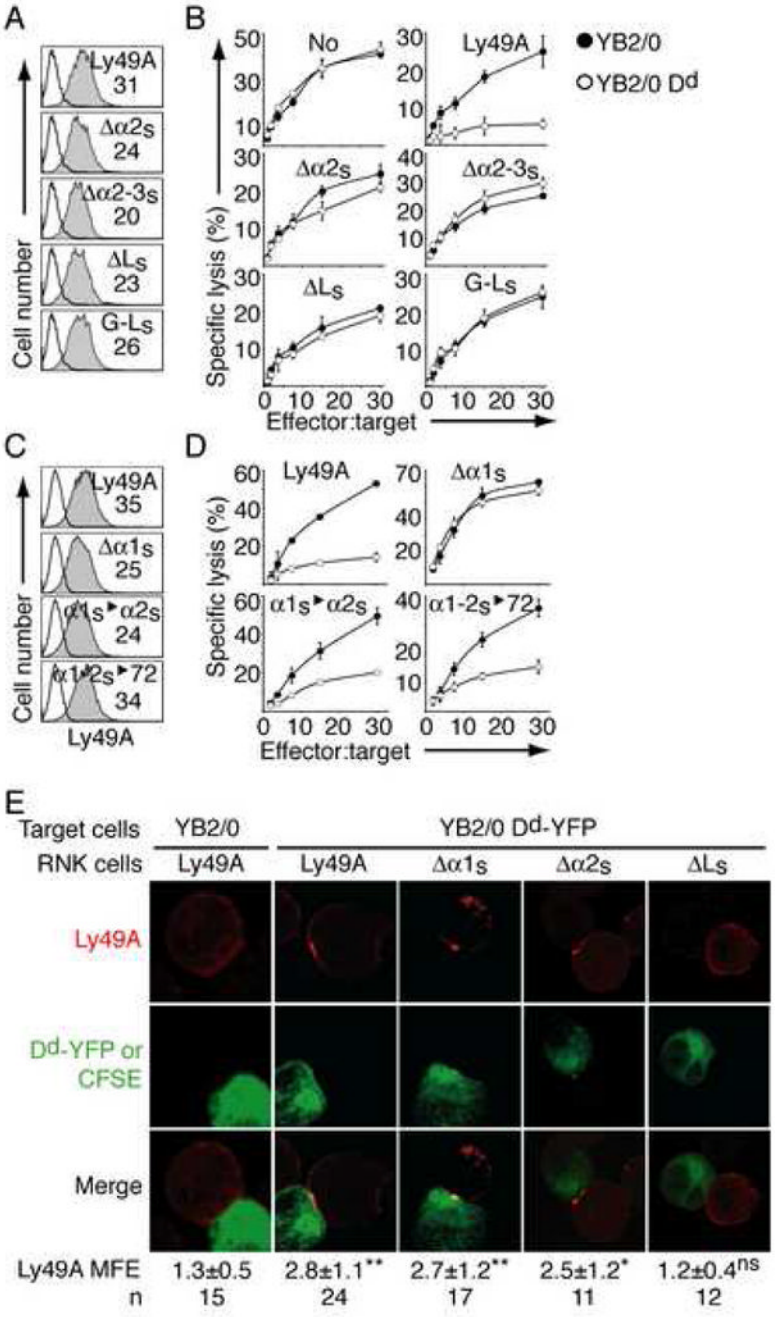

Figure 6.

Inhibitory Function and Accumulation at the Immune Synapse of Stalk Modified Ly49A Receptors. (**A,C**) RNK cells expressing no (open histograms) or the indicated Ly49A receptor (filled histograms) were stained with Ly49A mAb. Numbers indicate the MFI of staining. (**B,D**) RNK cells were used as effectors in lysis assays against untransfected (filled circles) and D^d-transfected (open circles) YB2/0 target cells (bottom). (**E**) YB2/0 cells, labeled with CFSE or expressing D^d-YFP (shown in green) were conjugated with the indicated RNK cells before staining for Ly49A (red). Microscopy images are maximum intensity projections of series of Z-stack confocal acquisitions. The intensity of Ly49A staining at the immune synapse relative to control regions, which do not make contacts, is referred to as the mean factor of

Ly49A enrichment (MFE). MFE values of >1 indicate Ly49A accumulation at the synapse. Differences in MFE values were evaluated relative to RNK Ly49A cells conjugated with control YB2/0 cells using the two-tailed student's t-test: *$p<0.05$; **$p<0.01$; ns, not significantly different. (n) Number of conjugates.

Table 1

Cis and *Trans* Interactions of Ly49A Stalk Variants with H-2D^d

C1498 transfectant		Ly49A levels[1] (% of wt)	Adhesion to D^{d+} cells[2] (% conjugates)	D^d tet / Ly49A[3] (% of wt)	Acid strip MFI D^d tet strip / n-strip[4]
No	D^d	0.4	10.1±3.9	na	na
Ly49A		100	58.0±8.4	100	1.1±0.2
Ly49A	D^d	78	**26.9±9.4**[5]	**40±10**	**3.4±0.8**
$\Delta\alpha1_S$ (Δ70-90)		113	53.5±12.1^{ns}	86±13	1.2±0.1
$\Delta\alpha1_S$	D^d	54	**20.6±8.2**	**15±4**	**8.1±1.0**
$\Delta\alpha2_S$ (Δ93-108)		93	52.6±9.6^{ns}	59±14	1.2±0.1
$\Delta\alpha2_S$	D^d	113	**21.0±7.3**	**22±9**	**4.4±0.9**
$\Delta\alpha3_S$ (Δ103-122)		176	30.7±5.2**	44±8	1.2±0.2
$\Delta\alpha3_S$	D^d	136	**19.5±6.5**	**19±3**	**2.6±0.2**
$\Delta\alpha1\text{-}2_S$ (Δ67-103)		72	10.5±4.7**	25±14	1.0±0.1
$\Delta\alpha1\text{-}2_S$	D^d	43	9.7±4.9	**5±2**	**2.5±0.3**
$\Delta\alpha2\text{-}3_S$ (Δ92-133)		44	5.9±4.6**	29±9	0.7±0.1
$\Delta\alpha2\text{-}3_S$	D^d	75	12.1±1.8	**11±6**	**3.2±0.5**
ΔL_S (Δ128-137)		246	49.2±5.3*	72±21	1.3±0.2
ΔL_S	D^d	246	43.7±3.3	73±20	1.5±0.4
G-L_S		260	33.1±6.1**	63±14	1.2±0.2
G-L_S	D^d	246	**25.0±4.0**	55±13	**2.2±0.4**

[1] Mean fluorescence intensity (MFI) of Ly49A staining using mAb JR9 relative to the staining of C1498 cells expressing wild type (wt) Ly49A (= 100%).

[2] Adhesion of Ly49A transfectants to C1498 cells expressing D^d. Numbers indicate the percentage of Ly49A cells that formed conjugates with D^d expressing cells. Statistical significance of differences in adhesion (*trans* binding) were determined relative to wild type Ly49A (in the absence of D^d co-expression) using the two-tailed students t-test:

* $p<0.05$;

** $p<0.01$, ns not significant.

[3] MFI of D^d tetramer (tet) staining relative to Ly49A (mAb JR9) staining normalized to the ratio obtained for C1498 cells expressing wild type (wt) Ly49A (= 100%).

[4] The MFI of D^d tetramer staining after acid treatment (strip) was divided by the value obtained before acid treatment (n-strip). Values of 1.0 indicate no change of D^d tet binding to Ly49A upon acid treatment. Values >1.0 indicate improved D^d tetramer binding upon acid stripping i.e. Ly49A has been masked by D^d expression in *cis*.

[5] Values indicated in bold face highlight statistically significant differences ($p<0.05$, based on two-tailed student's t-test) relative to the corresponding variant expressed in the absence of D^d (i.e. indicating *cis* interaction)

na not applicable

Values represent the mean (± SD) of 3-15 independent determinations.